DOI: 10.1002/adfm.200601034

Janus Nanoparticles by Interfacial Engineering**

By *Sulolit Pradhan*, *Li-Ping Xu*, and *Shaowei Chen**

Nanosized Janus particles were prepared by ligand exchange reactions of a Langmuir monolayer of hydrophobic alkanethiolate-passivated gold nanoparticles at relatively high surface pressures with hydrophilic thiol derivatives injected into the water subphase. The ligand intercalation between adjacent particles led to impeded interfacial mobility of the particles. Consequently, ligand place-exchange reactions were limited only to the side of the particles facing the water phase, leading to the formation of amphiphilic nanoparticles which exhibited hydrophobic characters on one side and hydrophilic on the other, analogous to the dual-face Roman god, Janus. The unique amphiphilic characters of the Janus particles were confirmed by a variety of experimental measurements, including contact angle measurements, FTIR, UV-visible, and NMR spectroscopies. Interestingly, the Janus particles might be dispersed in water, forming micelle-like aggregates, as revealed in dynamic light scattering and AFM measurements.

1. Introduction

The intense research interest in nanoscience and nanotechnology is largely fueled by the unique properties of nanoscale materials that may deviate vastly from those of their constituent atoms and bulk forms.[1] In order to exploit these unprecedented materials properties for the fabrication of next-generation devices and circuitries, two key aspects that are intimately related to each other have to be addressed: design and synthesis of nanoscale building blocks, and controlled assemblies of these structural units into functional architectures.[2] Thus, it is of critical importance to look for additional nanomaterials design parameters beyond size and shape. Among these, of particular interest is the creation of amphiphilic nanoparticles which exhibit hydrophobic characters on one side and hydrophilic on the other, akin to the dual-face Roman god, Janus.[3,4] These particles represent a unique nanoscale analog to the conventional surfactant molecules and thus may be exploited in the formation of functional superstructures by virtue of self-assembly.[5]

Most previous studies of Janus particles are focused on polymer-based materials.[6–10] Several effective routes have been reported towards the synthesis of these biphasic particles. For instance, microfluidic flow systems have been used to prepare amphiphilic particles by the polymerization of the Janus droplets formed within the microfluidic channels.[9,10] Submicron-sized Janus particles were prepared by biphasic electrified jetting of two polymer precursors.[7] In a different report,[8] Janus particles were prepared by sputtering gold onto the top face of a polymer bead array where further functionalization on the gold surface might be achieved. Paunov and co-workers[11] reported the fabrication of Janus particles by the replication of particle monolayers at liquid surfaces using a gel trapping technique. It should be noted that in these earlier studies, the typical sizes range from a few hundred nanometers to a few micrometers; and reports on the synthesis of nanometer-sized Janus particles[12] are actually rather scarce. In fact, the majority of nanometer-sized Janus particles refer to bifunctional heterodimers consisting of two different particle cores.[13,14] In these snowman or dumbbell-like nanostructures, the focus is generally placed on the core materials rather than on the organic capping shells. So the surface wettability of these hybrid particles may actually be very similar to that of their respective monomeric particles.

In the present investigation, we adopt the Langmuir method to create nanosized Janus particles that exhibit hydrophobic characters on one side and hydrophilic on the other, by taking alkanethiolate-protected nanoparticles[15] as the illustrating example. These particles represent a unique class of nanomaterials. They consist of a nanosized metal core on which alkanethiolates form a densely packed self-assembled monolayer by virtue of the strong affinity of the thiol group to transition metal surfaces. It has been demonstrated previously that ligand place-exchange reactions[16–20] (Scheme 1) can be employed to further functionalize the nanoparticle surface, which can then be used as a point of departure for more complicated surface functionalization, for instance, by surface coupling reactions. However, typically, in these earlier studies,[16–20] the particles and the new ligands are mixed in the same phase. Thus, while the final composition (up to 100 % displacement) of the particle surface layers can be controlled by the initial concentrations of the particles and the new ligands, the incorporation of

[*] Prof. S. Chen, S. Pradhan, Dr. L. Xu
Department of Chemistry and Biochemistry, University of California
Santa Cruz, California 95064 (USA)
E-mail: schen@chemistry.ucsc.edu

[**] This work was supported in part by the NSF (CAREER Award CHE-0456130), the ACS-PRF (39729-AC5M) and UCSC. Supporting Information is available including a representative Langmuir isotherm and additional AFM images of Janus nanoparticle aggregates.

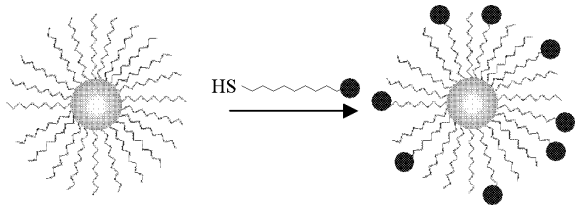

Scheme 1. Schematic of nanoparticle surface place exchange reactions.

the new ligands onto the particle surface is actually quite isotropic (it has been argued that the preferred sites are the core surface defects such as edges and vertexes which are distributed rather symmetrically on the nanoparticle surface[16–20]), resulting in structurally symmetrical particles as the products. This is primarily because of the equal accessibility of the entire particle surface to the new ligands in solution.

Therefore, in order to create nanosized Janus particles by ligand exchange reactions, the reactions must be confined to only one side of the particles. This can be achieved by dispersing the particles at an interface, e.g., at the air|water interface, where the particle interfacial mobility is impeded (e.g., by the Langmuir technique). Experimentally, as an illustrating example, the amphiphilicity was rendered to hexanethiolate-capped gold (AuC6) nanoparticles by subjecting them to place exchange reactions with hydrophilic mercaptopropanediol (MPD) at the air|water interface. First, the AuC6 particles were dispersed onto the water surface. Upon mechanical compression, a compact monolayer was formed with ligand intercalation between adjacent particles. With the introduction of MPD ligands into the water subphase, exchange reactions occurred which were limited only to the side of the particles in direct contact with the water phase, resulting in the formation of Janus nanoparticles. A wide array of experimental characterizations was then carried out to verify the amphiphilic structures.

2. Results and Discussion

In this study, Janus gold nanoparticles were prepared by exploiting the Langmuir technique (Scheme 2). Specifically, at low surface pressures, the hydrophobic alkanethiolate-protected particles are dispersed on the water surface with significant interfacial mobility, corresponding to the two-dimensional gas state (top panel). In contrast, upon mechanical compression, the nanoparticles will form a compact monolayer on the water surface. Importantly, at high surface pressures, because of ligand intercalation between adjacent nanoparticles, the interfacial mobility of the particles is significantly impeded (middle panel). By injecting a new ligand into the water subphase, ligand exchange reactions will occur at the particle surface that is in direct contact with the water phase, resulting in the formation of Janus nanoparticles (bottom panel).

Experimentally, prior to the injection of MPD ligands into the water subphase, the quality of the particle monolayer was evaluated by the corresponding Langmuir isotherm (a representative one was included in the Supporting Information).[21] In a typical experiment, the interparticle edge-to-edge distance was estimated by assuming a hexagonal close-packed structure of the particle monolayer[21] and controlled at 1.22 nm which was somewhat smaller than twice the hexanethiolate chain-length (0.77 nm each as estimated by Hyperchem®). Previous studies[21,22] have shown that by using particles of moderate dispersity (<20 %) a compact and long-range ordered monolayer could be formed on the water surface, where the interparticle separation (and hence surface pressure) could be readily regulated by simple mechanical compression.

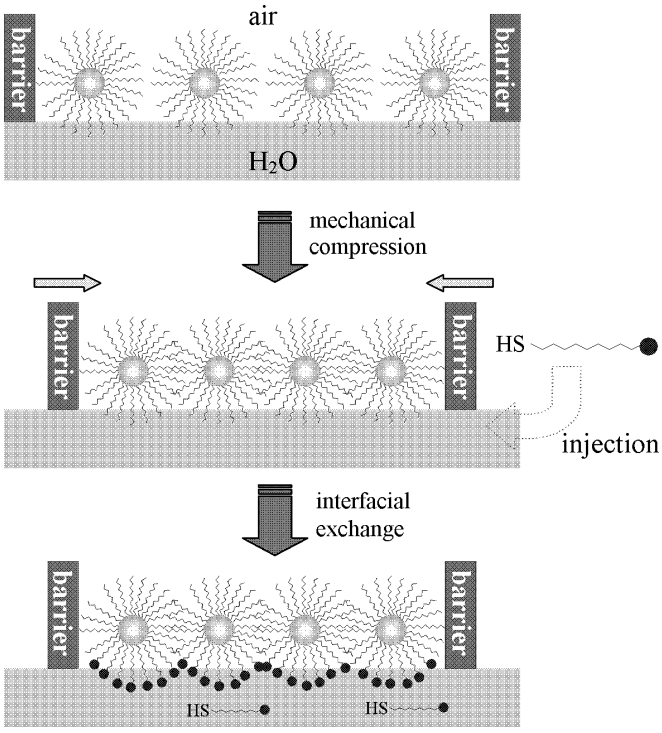

Scheme 2. Schematic of the preparation of Janus nanoparticles based on the Langmuir technique.

It should be noted that the same surface pressure was maintained for a few hours (typically 8 h) after the injection of MPD molecules into the water subphase (corresponding to a final concentration of 1 mM), where the exchange reactions were initiated with the bottom half of the particles. The resulting particles exhibited hydrophobic characters on the top half because of the original alkyl protecting ligands, whereas the MPD hydroxyl functionalities rendered the bottom half of the particles hydrophilic, hence the formation of Janus particles (Scheme 2).

The amphiphilic characters of the Janus particle surface were first examined by contact angle measurements of the particle monolayers deposited onto a substrate surface. Here two interfacial configurations were achieved by the Langmuir–Blodgett (LB) method (Scheme 3). In the up-stroke deposition, the hydrophilic face was in direct contact with the substrate whereas the hydrophilic face was exposed. In the down-stroke deposition, an opposite configuration was obtained. The correspond-

ADVANCED FUNCTIONAL MATERIALS

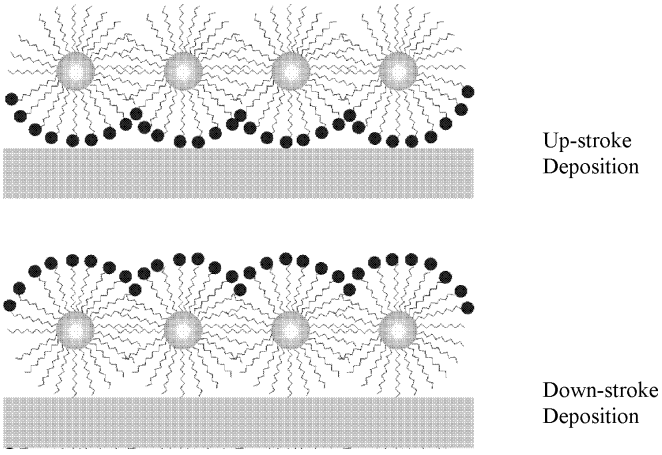

Scheme 3. Schematic of the interfacial configurations of the Janus nanoparticles in two LB depositions, up-stroke and down-stroke modes.

ing contact angles were then measured and compared, as summarized in Table 1. It can be seen that with the hydrophobic side exposed (up-stroke), the contact angle was averaged at 63.3° ± 2.7°, as compared to 53.4° ± 2.9° when the hydrophilic side was exposed (down-stroke). These values are very close to those observed with the self-assembled monolayers (SAMs) of hexanethiols and MPDs on a gold film surface, which are 63.1° ± 3.4°, and 50.5° ± 3.5°, respectively, suggesting the amphiphilic characters of the resulting particles.

Table 1. Contact angles of varied surface thin films.

	Up-stroke	Down-stroke
Janus particles[a]	63.3 ± 2.7°	53.4 ± 2.9°
Bulk-exchange particles[a]	58.5 ± 2.6°	58.0 ± 2.6°
AuC6 particles[a]	64.0 ± 2.8°	65.0 ± 2.6°
C6 SAM[b]	63.1 ± 3.4°	
MPD SAM[b]	50.5 ± 3.5°	
C6-MPD mixed SAM[b]	57.5 ± 3.2°	

[a] For the AuC6, Janus and bulk-exchange particles, the monolayers were deposited onto a glass slide surface by the LB technique.
[b] For the SAMs, the monolayers were formed on a gold film surface. In the mixed SAM, the molar ratio of C6SH and MPD was 1:1. All data shown were averaged from 8 measurements except for the Janus particles where 32 measurements were carried out.

To further verify the Janus structure, the contact angles of the bulk-exchange particles were also measured and compared. As anticipated from bulk-exchange reactions, the MPD ligands would be incorporated rather homogeneously onto the particle surface, thus the contact angles of the particle monolayers should be similar for the up-stroke and down-stroke deposition and in the intermediate range between those observed with the Janus nanoparticles. In fact, the contact angles were found to be 58.5° ± 2.6° and 58.0° ± 2.6°, respectively, for the bulk-exchange particle monolayers deposited by the up-stroke and down-stroke method (Table 1). Note that these are very comparable to that observed for a mixed SAM of C6SH and MPD (molar ratio 1:1) on a gold film surface, 57.5° ± 3.2°. Furthermore, the almost identical values of the two contact angles indicate very consistent wettability of the two particle faces because of the homogeneous distribution of the ligands on the particle surface, in sharp contrast to those with the Janus nanoparticles. Additional comparison can be made with the original AuC6 particles, where the corresponding LB monolayers exhibited a contact angle of 64.0° ± 2.8° and 65.0 ± 2.6° for the up-stroke and down-stroke deposition, respectively. Both values are very close to that of the C6SH SAM and of the Janus particle monolayer by the up-stroke deposition, but greater than those for the bulk-exchange particles.

Overall, these experimental results strongly suggest that the Langmuir-based approach (Scheme 2) is an effective route to the preparation of amphiphilic nanoparticles with distinctly different surface wettability.

The incorporation of the MPD ligands onto the particle surface was also verified by FTIR measurements. The Janus particles were collected from the water surface and purified by solvent extraction to remove excess of free ligands. Figure 1 shows the FTIR spectra of the AuC6 particles before and after interfacial exchange. It can be seen that the most remarkable discrepancy is the appearance of a broad peak centered at 3400 cm^{-1} for the Janus particles. This can be assigned to the vibrational stretch bands of the hydroxyl groups that are hydrogen-bonded between neighboring MPD molecules,[23] which is rather reasonable considering the close proximity of the hydroxyl moieties in the particle protecting layer. Additionally, the C–O stretching vibration band can also be clearly identified at 1030 cm^{-1}.[23]

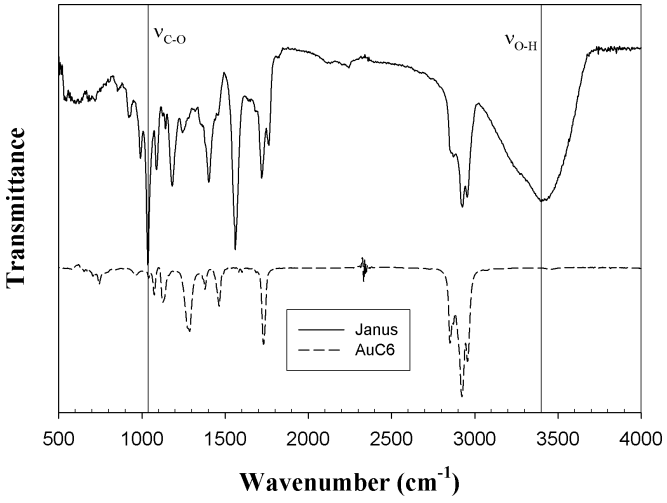

Figure 1. FTIR spectra of the AuC6 nanoparticles before and after interfacial exchange reactions with MPD ligands. The particle samples were prepared by dropcasting the respective solutions onto a CsBr plate.

To have a quantitative assessment of the surface composition of the Janus particles, NMR measurements were then carried out. Figure 2 depicts the ^{1}H NMR spectrum (in THF-d_4) of the

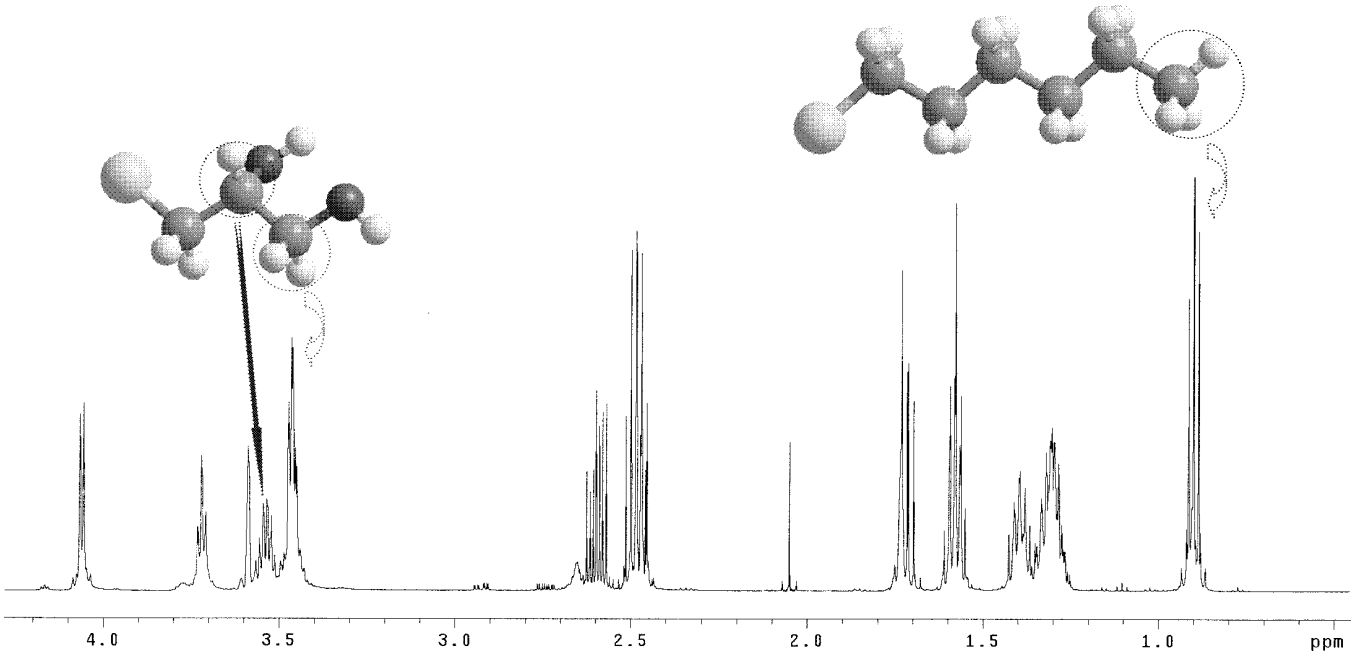

Figure 2. Proton NMR spectrum of the Janus nanoparticles after iodine desorption of the ligands from the particles.

surface protecting ligands after being desorbed from the particle surface by a minute amount of iodine. From the spectrum, the peak at 0.90 ppm is ascribed to the protons of the terminal methyl group of the hexanethiolate ligands, whereas the peaks at 3.45 ppm and 3.55 ppm are attributable to the methylene and methylyne protons next to the hydroxyl group in the MPD ligands, respectively. From the ratio of the integrated peak areas of these protons, one can estimate that about 48.9 % of the original hexanethiolate ligands were replaced by the new MPD molecules. The fact that about half of the ligands were hydrophobic and the other half, hydrophilic, is again in agreement with the amphiphilic structure of the Janus particles.

The same method was also applied to the bulk-exchange particles in which the percentage of MPD and C6SH ligands were found to be 51.7 % and 48.3 %, respectively (spectrum not shown). In addition, by comparing the NMR profiles of the Janus and bulk-exchange particles with those of free MPD and C6SH ligands, it was found that the samples were free of impurities and all the peaks observed were characteristic of the two ligands. As the original AuC6 particles exhibit a molecular composition of $Au_{314}(C6)_{91}$, the resulting Janus and bulk-exchange particles can be approximated as $Au_{314}(C6)_{46.5}(MPD)_{44.5}$, and $Au_{314}(C6)_{44}(MPD)_{47}$, respectively.[24]

UV-vis measurements were also carried out to provide further insights into the amphiphilic characters of these Janus particles. Figure 3A shows the optical absorption profiles of the AuC6 particles before (in CH_2Cl_2, solid curve) and after interfacial exchange (in THF, dotted curve), both of which are very similar in appearance. Because of the small core size, the particles only exhibited an exponential decay response (Mie scattering) with a small and broad peak at ca. 520 nm (as determined by the 2nd-order derivatives of the absorption profiles), characteristic of the surface plasmon resonance of nanosized gold particles.[25–27] However, for the Janus particles dissolved in THF, upon the addition of an equal amount of water, the solution remained transparent. Even after extensive bubbling of the solution by UHP nitrogen to remove the THF solvent, no apparent agglomeration was observed. The corresponding UV-vis absorption spectra are shown in dashed and dashed/double-dotted lines, respectively. The fact that the particles remained stable in water suggests that the particles might adopt a micellar superstructure as a consequence of the amphiphilic characters, akin to the conventional surfactant molecules. Such a hypothesis is also supported by the increasingly pronounced absorption peak of the particle surface plasmon resonance and its red-shift to 562 nm in the binary mixture of water and THF, and 600 nm in water alone, which can be accounted for by the close proximity of the particles in the aggregates that leads to enhanced interparticle electronic coupling.[25–27]

While bulk-exchange particles exhibited similar solubility properties in organic media, the stability of the particles in water alone was not as good as that of the Janus nanoparticles. For instance, the Janus particles were found to be stable in water for more than 8 hrs whereas the bulk-exchange particles started to precipitate out from the solution in about 2 h, as manifested in UV-vis measurements (Fig. 3B and C). One can see that the UV-vis absorption profiles of the Janus nanoparticles in water (panel B) remained practically unchanged for 8 h whereas after 6 h, significant precipitation occurred with the bulk-exchange particles and the optical absorbance diminished substantially (panel C). The appearance of two absorption peaks at 570 and 690 nm in the spectra of bulk-exchange particles in water (panel C) might be attributable to the formation

ADVANCED FUNCTIONAL MATERIALS

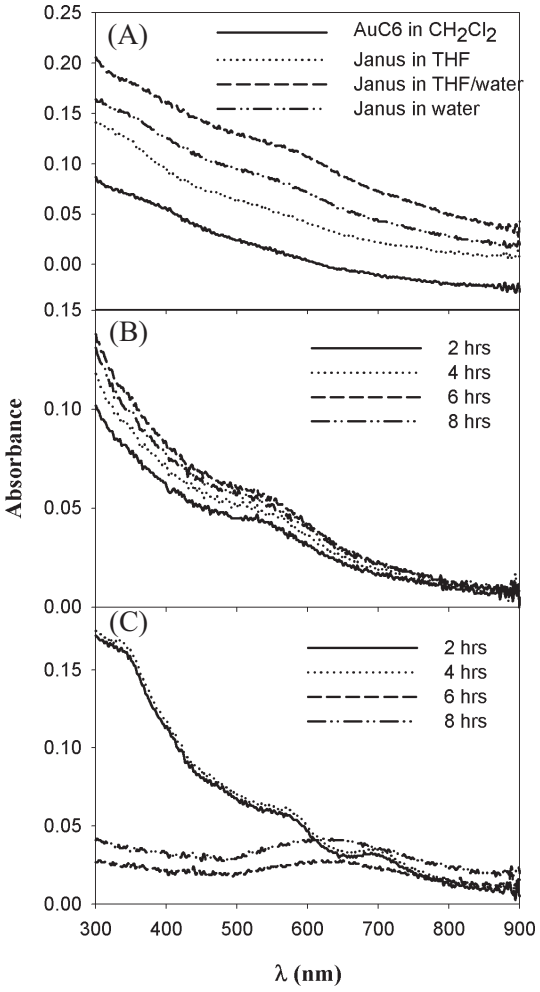

Figure 3. A) UV-visible spectra of the particles before and after interfacial exchange reactions with MPD ligands. The particle concentration was ca. 1 mg mL^{-1}. These include the spectra of the Janus particles dissolved in THF followed by the addition of an equal amount of water, as well as that where THF was removed by extensive bubbling with nitrogen. Note that the spectra were offset for clarity purpose. Also shown are the UV-vis absorption spectra of the Janus nanoparticles (B) and bulk-exchange particles (C) in water at different times after the removal of THF.

of particle aggregates of different morphologies (shape), in contrast to the Janus particles where the particle aggregates were likely to be micelle-like.

The average sizes of the aggregate structures of the Janus and bulk-exchange particles in these different solvents were then evaluated by dynamic light scattering (DLS) measurements. The results were summarized in Table 2. It is interesting to note that in THF, the bulk-exchange nanoparticles essentially behave individually with the measured size (2.4 nm) consistent with the particle physical diameter. As the MPD ligands are uniformly distributed on the particle surface, the overall particle solubility may be mainly determined by the longer hexanethiolates, thus leading to good dispersity of the particles in THF. In contrast, for the Janus nanoparticles, the formation of aggregates in THF of the order of 269 nm was found. This may be ascribed to the amphiphilic nature of the particles that

Table 2. Average size of the particle aggregates in different solvents by DLS measurements.

Solvent	Janus Particles [nm]	Bulk-exchange particles [nm]
THF	269.0	2.4
THF/H_2O (50:50)	253.0	64.0
H_2O	307.0	171.0

self-assembled to minimize the exposure of the hydrophilic face to the solvent. Upon the addition of an equal volume of water into the solutions, aggregation of the bulk-exchange particles started to occur with an average size of 64 nm; whereas the aggregates of the Janus nanoparticle only saw a small decrease of the average size to 253 nm. With the removal of THF from the particle solutions, the aggregates of the bulk-exchange particles increased to 171 nm whereas those of the Janus particles increased to 307 nm. Overall, the Janus particles maintained a more steady aggregated form of structures in different solvents, most probably as a consequence of the amphiphilic nature of the particles that rendered it energetically favorable to arrange the assembling of the particles in different solvents so as to maintain a large aggregation of the particles, whereas the solubility of the bulk-exchange particles was more sensitive to the specific solvent medium where the large energy costs of particle solvation led to the formation of only small particle aggregates because of the homogeneous distribution of the hydrophilic and hydrophobic ligands on the particle surface.

More importantly, by casting a drop of the water solution onto a mica substrate, AFM measurements revealed numerous aggregates with varied cross-sectional dimensions and height (Fig. 4), in good agreement with the above DLS measurements. Figure 4A depicts a typical AFM image acquired in tapping mode, in which several particle aggregates can be observed; and from the line scans, we can estimate that the lateral dimension of the aggregates is about 400 nm across with a rather flat height of 10–5 nm which corresponds to 3 to 5 stacked layers of particles. Note that from DLS studies (Table 2), the average size of the particle aggregates was about 300 nm. Thus, it is plausible that the particles adopted a structure that was analogous to liposomes in water (Scheme 4).

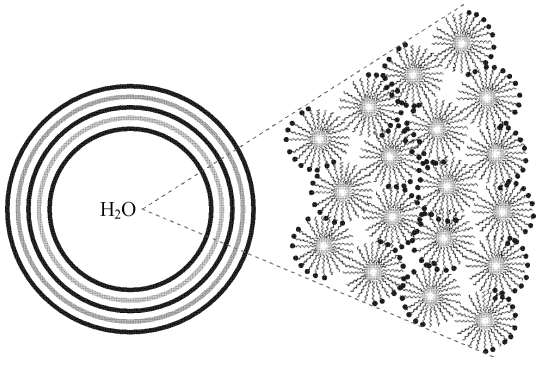

Scheme 4. Schematic of the particle aggregates in water.

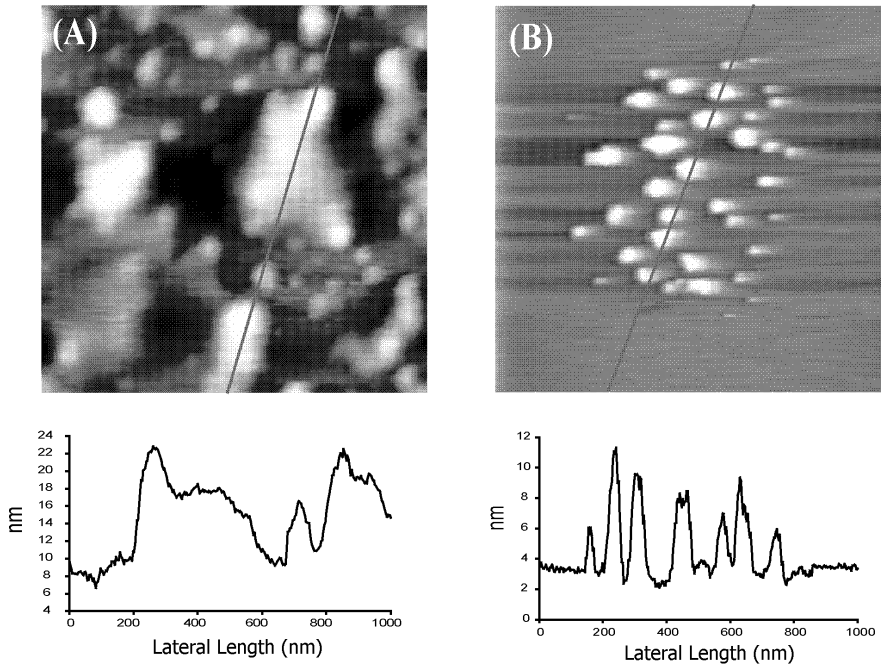

Figure 4. AFM images of the Janus particles suspended in water (concentration 0.19 mM) which were acquired in varied operation modes: A) tapping mode; and B) contact mode. The bottom panels are the corresponding line scan profiles. The samples were prepared by dropcasting the water suspension onto a freshly cleaved mica surface. Scan size 1000 nm × 1000 nm; and scan rate 2 lines/s.

When deposited onto the substrate surface for AFM measurements, the aggregates crashed, resulting in the appearance of a pancake-like structure (Fig. 4A). We also examined the particle aggregates with contact mode AFM and a representative image was shown in Figure 4B, where it can be seen that the lateral dimension is drastically reduced to be less than 100 nm, with height ca. 6 nm. The drastic diminishment of the particle aggregates might be accounted for by at least two factors. First, in contact mode, because of the excessive force, the top layers of the particle aggregates might be shaved off thus revealing the "interior" details of the aggregates—the streaks seen in the images (Fig. 4B) most probably arose from the strong interactions between the tip and the substrate.[28] Consequently, the particle aggregates disintegrated into smaller ones. Second, the effective height of the aggregates measured in contact mode may also appear smaller because of tip penetration into the particle protecting layers and tip pushing of the particles toward the substrate. Consequently, the height measured most probably does not reflect the contribution of the particle surface ligands. In contrast, in tapping mode, the probe tip intermittently makes contact with the sample surface. Thus, contributions from the particle surface ligand layer must be taken into account.

Further studies of the aggregation behaviors of the Janus particles were carried out by varying the particle concentration in water. The corresponding AFM images were included in the Supporting Information. It was found that the number and size of the particle aggregates decreases with decreasing particle concentration. For instance, as shown above (Fig. 4A), at the concentration of 0.19 mM, the size of largest particle aggregates is about 440 nm × 230 nm and the height 15 nm; whereas at 0.16 mM, the largest aggregate is about 160 nm × 180 nm; and at an even lower concentration, 0.11 mM, particle aggregates became significantly less populous with the dimension also reduced to 90 nm × 180 nm. This suggests that a minimum concentration is required for the formation of particle aggregates, analogous to the critical micelle concentration (CMC) observed in conventional surfactant molecules.[5]

In sharp contrast, for the original (unexchanged) AuC6 particles, upon the addition of an equal amount of water into the solution (also in THF), the particles precipitated out immediately forming some black flaky solids at the bottom of the container.

More recently, we measured the adhesion force interactions between an unmodified silicon AFM tip and the Janus nanoparticles deposited onto substrate surfaces with different surface wettability, and found that when the hydrophilic face of the particles was exposed, the adhesion force was substantially greater than that with the hydrophobic face exposed.[29] This further confirms the amphiphilic nature of the Janus nanoparticles.

3. Conclusions

A simple and yet effective approach based on interfacial engineering to the preparation of amphiphilic nanoparticles was presented. The resulting nanoparticles consisted of ca. 50 % hydrophobic and 50 % hydrophilic ligands on the particle surface which were distributed on two separate sides of the particles. Consequently, the particles behave similarly to the conventional surfactant molecules, as revealed in DLS and AFM measurements. Using the strategy presented above as a point of departure, it is anticipated that the Janus nanoparticles may be exploited for the fabrication of more complicated and functional nanoarchitectures by deliberate selection of the chemical ligands.

Currently there remain two challenges in the preparation of Janus nanoparticles. The first is to scale up the synthesis; and the other is to maintain the long-term structural integrity of the Janus characters of the particles because of ligand diffusion on the particle surface. These issues are being pursued and results will be reported in due course.

ADVANCED FUNCTIONAL MATERIALS

4. Experimental

Chemicals: Hydrogen tetrachloroauric acid ($HAuCl_4 \cdot xH_2O$) were synthesized by dissolving ultra-high purity gold (99.999 %, Johnson Matthey) in freshly prepared aqua regia followed by crystallization [30]. Tetraoctylammonium bromide (Alfa Aesar, 98 %), hexanethiol (C6SH, Acros, 96 %), sodium borohydride ($NaBH_4$, Acros, 99 %), toluene (Acros, 99 %), ethanol (Fischer, 100 %), dichloromethane (CH_2Cl_2, Fischer, 99.9 %), tetrahydrofuran (THF, Acros, 99 %), deuterized tetrahydrofuran (THF-d_4, Acros, 99.5 %), and 3-mercaptopropane-1,2-diol (MPD, Aldrich, 95 %) were all used as received. Other solvents were purchased from typical commercial sources at their highest purities and used without further treatments. Water was supplied by a Barnstead Nanopure water system (18.3 MΩ).

Particle Synthesis: The AuC6 particles are synthesized by using the Brust protocol [15]. The particles then underwent careful fractionation by using a binary solvent-nonsolvent mixture of toluene and ethanol [16,31] and thermal annealing in toluene [32] at 110 °C for 8 h in an oil bath to reduce the core size dispersity, and the fraction with average core diameter of 2.0 nm and core size dispersity of ca. 20 % (as determined by transmission electron microscopic measurements, with the particle composition [24] approximated as $Au_{314}(C6)_{91}$) was used in the subsequent measurements.

Langmuir Monolayers: Monolayers of the AuC6 nanoparticles were then created by using a Langmuir–Blodgett trough (NIMA Technology, Model 611D) [21]. In a typical experiment, 300 μL of the AuC6 particle solution at a concentration of 1 mg mL^{-1} in toluene was spread in a dropwise fashion onto the water surface using a Hamilton microliter syringe. At least one hour was allowed for solvent evaporation and between compression cycles. The barrier speed was controlled at 10 cm^2 min^{-1}.

To prepare the Janus nanoparticles, the particle monolayer was compressed to a desired surface pressure where the interparticle edge-to-edge separation was maintained at a value smaller than twice the extended ligand chainlength. This resulted in ligand intercalation between adjacent particles and hence impeded the interfacial mobility of the particles. At this point, a calculated amount of MPD ligands was injected into the water subphase by using a Hamilton microliter syringe. The particles were kept at the same surface pressure for an extended period of time (typically 8 h) before the particles were either deposited onto a substrate or collected by a Pasteur pipette. Note that at least four batches of samples prepared under identical conditions were collected so that there were enough materials for further analyses. As inevitably a small amount of water and free MPD ligands were also sucked into the pipet, these excessive MPD ligands were removed by solvent extraction with the addition of dichloromethane to the solution, where the particles were dissolved in dichloromethane and the MPD ligands in water, as manifested by the appearance of a colorless water phase and an organic phase in light brown color. It was found that the resulting particles were soluble in CH_2Cl_2 and THF, but not directly in water without agitation.

As a control experiment, MPD-functionalized nanoparticles were also prepared by bulk exchange reactions (Scheme 1) where a calculated amount of AuC6 nanoparticles and MPD ligands was co-dissolved in THF under vigorous magnetic stirring for two days (with the eventual MPD:C6 ratio on the particle surface similar to that of the Janus particles). The solution was then dried by a rotary evaporator at reduced pressure and excessive free ligands were removed by extensive rinsing with ethanol. The resulting particles were denoted as bulk-exchange particles and, similar to the Janus nanoparticles, were soluble in THF and CH_2Cl_2, but not directly in water without agitation.

Contact Angle Measurements: Contact angle measurements of the Langmuir–Blodgett (LB) monolayers of the resulting Janus nanoparticles were carried out with a Tantec CAM-PLUS Contact Angle Meter. Prior to deposition, a flat glass substrate was cleansed in aqua regia followed by extensive rinsing with Nanopure water, and ethanol. It was then blow-dried by ultra-high-purity (UHP) nitrogen. The particle monolayer films were deposited onto the glass substrate by the LB technique (the dipper speed was generally controlled at 1 mm min^{-1}) in two different configurations. In the up-stroke mode, the hydrophilic face of the particles was anticipated to be in direct contact with the substrate whereas the hydrophobic face was exposed as the top. An opposite configuration was achieved in the down-stroke deposition. At least 8 contact angles were acquired in each deposited film. To eliminate possible contamination of free MPD ligands in the particle monolayer films, the glass slides with the deposited particle films were first rinsed with a copious amount of water and ethanol, and then dried in a gentle stream of UHP nitrogen, prior to contact angle measurements.

The depositions of the bulk-exchange particles and the original AuC6 particles were carried out in a similar fashion except that as no MPD ligands were injected into the water subphase, no post-deposition rinsing was done before the contact angles were measured.

Spectroscopies: FTIR measurements of the particles were performed with a Perkin-Elmer Precision Spectrum-1 FTIR Spectrometer. The particles were first dissolved in dichloromethane and a thick film was formed by dropcasting the solution onto a CsBr plate. The sample was then dried in a gentle stream of UHP nitrogen. The UV-visible spectra were collected with a UNICAM ATI UV4 spectrometer at a particle concentration of ca. 1 mg mL^{-1} in dichloromethane using a 1 cm quartz cuvette.

To quantitatively evaluate the surface composition of the Janus and bulk-exchange particles, the particles were first dissolved in THF-d_4. Then a minute amount of iodine was added into the solution which led to the desorption of the thiol ligands from the Au core surface. ^{1}H NMR spectra were then collected with a Varian Unity 500 MHz spectrometer.

To verify the formation of higher-order aggregate structures of the resulting particles when dissolved in THF, water, or THF/water mixtures, dynamic light scattering (DLS) measurements were carried out with a ProteinSolution *Dynapro* Temperature Controlled Microsampler. Typically a sample aliquot (12 μL) of the particle solutions at a concentration of 0.1 mg mL^{-1} in THF was introduced into a sample holder using a 20 μL Eppendorf pipette. The results were reported in terms of % mass.

AFM Measurements: AFM images were acquired under ambient conditions with a Molecular Imaging PicoLE SPM instrument in tapping and contact modes. In tapping mode measurements, the cantilevers exhibited resonant frequencies between 120 and 190 kHz, force constants of 2.5–8.5 N m^{-1}, and a tip apex radius of approximately 10 nm. In contact mode measurements, ultrasharp silicon cantilevers were used with the resonant frequencies between 8.5 and 15 kHz, force constants of 0.05–0.30 N m^{-1} and a tip curvature radius of ~10 nm. The resulting images were flattened and plane-fit using Molecular Imaging software. The samples for AFM measurements were prepared by dropcasting the aqueous solution of the Janus nanoparticles onto a freshly cleaved mica, followed by solvent evaporation at ambient temperature.

Received: October 31, 2006
Revised: March 5, 2007
Published online: August 9, 2007

[1] G. Schmid, *Chem. Rev.* **1992**, *92*, 1709.
[2] J. Z. Zhang, Z. L. Wang, J. Liu, S. W. Chen, G.-y. Liu, *Self-Assembled Nanostructures*, Kluwer Academic/Plenum Publishers, New York **2003**.
[3] C. Casagrande, M. Veyssie, *C. R. Acad. Sci. Ser. Ii* **1988**, *306*, 1423.
[4] P. G. Degennes, *Science* **1992**, *256*, 495.
[5] A. Ulman, *An Introduction to Ultrathin Organic Films: from Langmuir–Blodgett to Self-Assembly*, Academic, Boston **1991**.
[6] A. Perro, S. Reculusa, S. Ravaine, E. B. Bourgeat-Lami, E. Duguet, *J. Mater. Chem.* **2005**, *15*, 3745.
[7] K. H. Roh, D. C. Martin, J. Lahann, *Nat. Mater.* **2005**, *4*, 759.
[8] D. Suzuki, H. Kawaguchi, *Colloid Polym. Sci.* **2006**, *284*, 1471.
[9] Z. H. Nie, W. Li, M. Seo, S. Q. Xu, E. Kumacheva, *J. Am. Chem. Soc.* **2006**, *128*, 9408.

[10] T. Nisisako, T. Torii, T. Takahashi, Y. Takizawa, *Adv. Mater.* **2006**, *18*, 1152.
[11] V. N. Paunov, O. J. Cayre, *Adv. Mater.* **2004**, *16*, 788.
[12] A. Perro, S. Reculusa, F. Pereira, M. H. Delville, C. Mingotaud, E. Duguet, E. Bourgeat-Lami, S. Ravaine, *Chem. Commun.* **2005**, 5542.
[13] H. W. Gu, R. K. Zheng, X. X. Zhang, B. Xu, *J. Am. Chem. Soc.* **2004**, *126*, 5664.
[14] Y. Q. Li, G. Zhang, A. V. Nurmikko, S. H. Sun, *Nano Lett.* **2005**, *5*, 1689.
[15] M. Brust, M. Walker, D. Bethell, D. J. Schiffrin, R. Whyman, *J. Chem. Soc. Chem. Commun.* **1994**, 801.
[16] A. C. Templeton, M. P. Wuelfing, R. W. Murray, *Acc. Chem. Res.* **2000**, *33*, 27.
[17] M. G. Warner, S. M. Reed, J. E. Hutchison, *Chem. Mater.* **2000**, *12*, 3316.
[18] R. Shenhar, V. M. Rotello, *Acc. Chem. Res.* **2003**, *36*, 549.
[19] H. Wellsted, E. Sitsen, A. Caragheorgheopol, V. Chechik, *Anal. Chem.* **2004**, *76*, 2010.
[20] A. R. Rothrock, R. L. Donkers, M. H. Schoenfisch, *J. Am. Chem. Soc.* **2005**, *127*, 9362.
[21] S. W. Chen, *Langmuir* **2001**, *17*, 6664.
[22] J. R. Heath, C. M. Knobler, D. V. Leff, *J. Phys. Chem. B* **1997**, *101*, 189.
[23] R. M. Silverstein, G. C. Bassler, T. C. Morrill, *Spectrometric Identification of Organic Compounds*, Wiley, New York **1991**.
[24] M. J. Hostetler, J. E. Wingate, C. J. Zhong, J. E. Harris, R. W. Vachet, M. R. Clark, J. D. Londono, S. J. Green, J. J. Stokes, G. D. Wignall, G. L. Glish, M. D. Porter, N. D. Evans, R. W. Murray, *Langmuir* **1998**, *14*, 17.
[25] C. F. Bohren, D. R. Huffman, *Absorption and Scattering of Light by Small Particles*, Wiley, New York **1983**.
[26] S. Underwood, P. Mulvaney, *Langmuir* **1994**, *10*, 3427.
[27] M. M. Alvarez, J. T. Khoury, T. G. Schaaff, M. N. Shafigullin, I. Vezmar, R. L. Whetten, *J. Phys. Chem. B* **1997**, *101*, 3706.
[28] K. C. Grabar, K. R. Brown, C. D. Keating, S. J. Stranick, S. L. Tang, M. J. Natan, *Anal. Chem.* **1997**, *69*, 471.
[29] L. Xu, S. Pradhan, S. W. Chen, *Langmuir*, in press.
[30] G. Brauer, *Handbook of Preparative Inorganic Chemistry*, Academic, New York **1963**.
[31] R. L. Whetten, M. N. Shafigullin, J. T. Khoury, T. G. Schaaff, I. Vezmar, M. M. Alvarez, A. Wilkinson, *Acc. Chem. Res.* **1999**, *32*, 397.
[32] S. W. Chen, *Langmuir* **2001**, *17*, 2878.